Hygrothermal aging of mastic samples

S. Khalighi, L. MA, R. Koning, & A. Varveri Delft University of Technology, Netherlands

ABSTRACT: This study examines the aging behavior of mastic samples subjected to hygrothermal conditions in a pressure aging vessel (PAV) for 10, 20, and 40 hours, as well as to reactive oxygen species and humidity in Vienna Binder Aging (VBA-WET). Fourier-transform infrared spectroscopy (FTIR) was used to analyze the chemical aging processes, and principal component analysis (PCA) was applied to differentiate mastic types and evaluate the efficacy of indices versus spectral data. Results show that W60k mastic has lower carbonyl index and smaller increase of sulfoxide index, indicating greater resistance to oxidative degradation compared to W mastic. PCA effectively differentiates the mastic types and confirms that both FTIR indices and full spectra distinguish between mastic types. These findings highlight the impact of filler composition on aging behavior and suggest directions for future research on material performance in practical applications.

1 INTRODUCTION

The aging process of bituminous binders is crucial for the longevity of asphalt pavements, as excessive aging can significantly impair the durability of asphalt mixtures. Aging occurs in two phases: shortterm aging during storage, mixing, and paving, and long-term aging that occurs in service (Petersen 2009). Key mechanisms such as oxidation, evaporation of volatile components, and steric hindrance drive these processes, with oxidative aging having a particularly pronounced impact on long-term pavement performance. Standard aging protocols, including the Rolling Thin Film Oven (RTFO) and Pressure Aging Vessel (PAV), have been established to simulate these conditions (Migliori and Corté 1998, Airey 2003). However, these aging protocols have been proven to be not accurate enough in simulating field asphalt pavement aging (Singhvi et al. 2022). To improve laboratory protocols and better mimic field conditions, it is essential to understand the effect of mineral fillers and the effects of environmental factors such as pressure, moisture, and reactive oxygen species (ROS) (Khalighi et al. 2024a).

Fillers significantly influence the aging behaviour of asphalt binders, affecting both their chemical and physical properties. Previous studies indicate that fillers like hydrated lime can retard aging more effectively than other materials, limiting oxygen diffusion and reducing viscosity and softening point increases (Gubler et al. 1999, Alfaqawi et al. 2022). Additionally, environmental factors, including pressure and moisture, also play a vital role in the aging process, with the combination of these elements requiring careful examination to develop more representative aging protocols. This study aims to investigate the responses of mastics containing hydrated

lime and limestone to aging in PAV under humidity and heat (hygrothermal aging) (Khalighi et al. 2024a) and VBA (Khalighi et al. 2024b), utilizing Fourier-transform infrared spectroscopy (FTIR) (Khalighi et al. 2024c) and principal component analysis (PCA) (Ma et al. 2023) to assess and compare aging behaviours at the mastic level.

2 MATERIALS AND METHODS

2.1 Materials and sample preparation

In this study, one PEN 70/100 bituminous binder was evaluated, named as Q, which has a softening point between 43-51 °C. Its complex shear modulus at 1.6 Hz and 60 °C is 1.8 kPa, with a phase angle of 88° under the same conditions. The elemental comincludes nitrogen (0.59%),position (79.19%), hydrogen (10.81%), sulfur (4.47%), and oxygen (2.25%). For mastics, two types were prepared using different fillers: Wigro (limestone) and Wigro60k (hydrated lime), with a filler-to-binder ratio of 1:1 (wt%). Both fillers, from the lime family, are widely used in the Netherlands. The specifications for fillers can be found in (Mastoras et al. 2021). Both components were preheated to 130 °C for one hour, then mixed and stirred for five minutes. The mixture was then oven-cured at 130°C for 30 minutes and manually stirred for even distribution of filler.

Mastic samples were prepared by pouring fresh mastics into pans, forming films of 3.2 mm thickness. The material required for film preparation varies with filler density. Calculation details are in (Mastoras et al. 2021). Short-term aging was conducted at 163°C for 5 hours per EN 12607-2 (EN 12607-2 2014). Portions of the aged binders were

then transferred to glass petri dishes to achieve a uniform 1 mm thickness by reheating at 163°C for 3 minutes. Uniform filler-binder blending was ensured by thorough mixing after each step.

2.2 Long-term aging conditions

The LTA conditions involved PAV treatment at 85°C for varying durations (10, 20, 40 hours) and 99% relative humidity, using 1000 grams of demineralized water to achieve this (Khalighi et al. 2024a). Additionally, the Viennese Binder Aging (VBA) method was employed, exposing samples to air with 25 ppm NO2 and 4 g/m³ ozone at 85 ± 1°C for three days, along with 75 g/m³ humidity (VBA-Wet) (Mirwald et al. 2020). Naming conventions include "W"/"W60k" for Wigro/Wigro60k, "VBA-W" for hygrothermal aging in VBA, and "W-10H" for hygrothermal aging in PAV for 10 hours.

2.3 Fourier-transform infrared spectroscopy (FTIR)

Chemical changes in mastic samples during aging were analysed using ATR-FTIR spectroscopy. Samples (~1 g) were heated to 110°C, stirred, and deposited on silicon foil for analysis with a Nicolet iS5 Thermo Fisher Scientific instrument, generating four spectra per aging state in the 4000–400 cm⁻¹ range. Pre-processing included an 8-point baseline correction and normalization via the NMO method (Khalighi et al. 2024c). Table 3 lists the wavenumber ranges of main functional groups identified for mastic samples. Functional group indices were calculated using the equation:

$$index = A_x / A_{Total}$$
 (1)

$$A_{\text{Total}} = A_{810} + A_{1030} + A_{1376} + A_{1460} + A_{1600} + A_{1700} + A_{2953} + A_{3400}$$
 (2)

Where A_x represents the tangential peak area under the curve within specified ranges from Table 1.

Table 1. Main functional groups of mastic in FTIR spectra (Khalighi et al. 2025).

Area groups	Vertical band	I limit (cm ⁻¹) Functional		
A810	680-912	(CH ₂) _n , thiols, CO ₃ ²⁻		
A1030	930-1120	S=O, silicate		
A1376	1350-1395	Branched aliphatic structures		
A1460	1395-1525	CH ₃ and CH ₂ , CO ₃ ²⁻		
A1600	1550-1660	Aromatic structure,C=C		
A1700	1660-1735	Carbonyl, C=O		
A2953	2820-2990	Aliphatic structures		
A3400	3100-3700	Hydroxyl stretching, OH, NH		

2.4 Principle component analysis (PCA)

PCA is a crucial method for transforming datasets with many variables into uncorrelated components, aiding in dimensionality reduction. The scores for target samples are calculated using $Y = X \times W$, where \mathbf{X} is the dataset of m samples across l categories and n variables. The matrix W, an $n \times p$ loading matrix, indicates the selected principal components, while Y forms an $m \times p$ score matrix projecting X into a p-dimensional feature space. W is derived from the eigenvectors and eigenvalues of the covariance matrix of the spectral dataset, with the largest eigenvalues selected to construct W. PCA loadings are further analyzed to identify significant regions for cluster formation (Ma et al. 2023). The dataset for PCA included FTIR results, encompassing all indices listed in Table 1, and an additional analysis utilized the entire FTIR spectra for comparison.

3 RESULT AND DISCUSSION

3.1 Effect of Aging on Mastic Samples using FTIR

Figure 1 shows the pre-processed FTIR spectra of mastic samples subjected to hygrothermal aging in PAV and VBA. Notably, certain spectral regions, particularly the fingerprint region, exhibit an upward shift with aging. To quantify these changes, the areas under the key peaks will be analysed according to the regions specified in Table 1. Previous studies have identified the carbonyl, sulfoxide, hydroxyl, and long-chain indices in the 680-734 cm⁻¹ and 783-838 cm⁻¹ regions as significant for mastic differentiation and aging (Khalighi et al. 2025). Consequently, these indices will be the primary focus of the analysis.

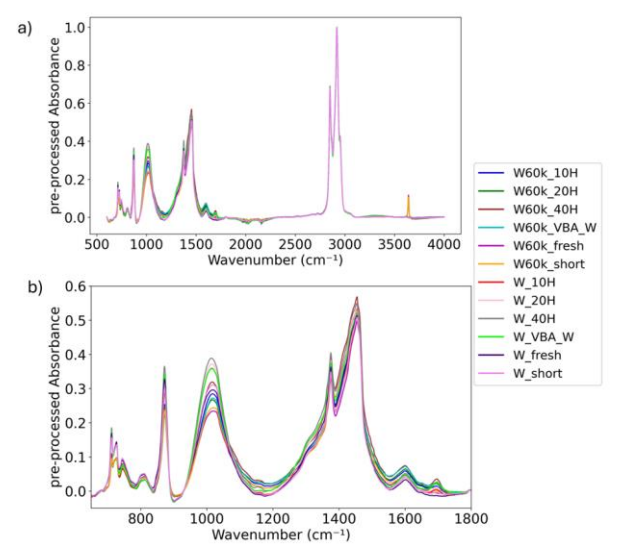
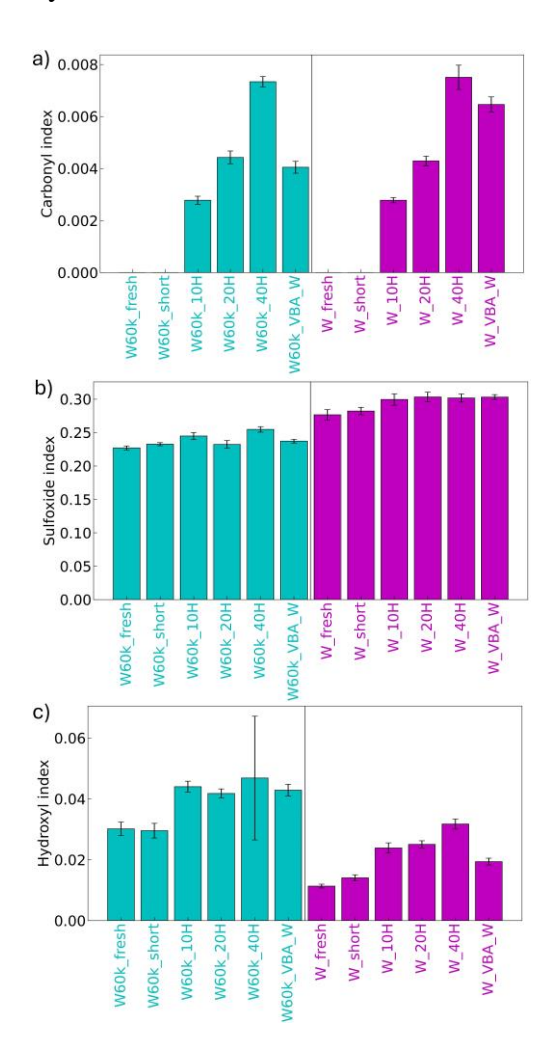


Figure 1- FTIR spectra of fresh, short-term aged, and long-term aged mastics under various hygrothermal aging conditions in PAV (10, 20, and 40 hours) and VBA-WET: a) pre-processed spectra; c) variations in the 650-1800 cm⁻¹ fingerprint region.

Figure 2a illustrates the carbonyl index, which increases with long-term aging, indicating the formation of oxidative products. Notably, hygrothermal aging under PAV conditions, particularly at 40 hours, results in a more significant increase in the carbonyl index compared to 72 hours of VBA-WET aging, underscoring the role of high pressure in oxidative degradation. Figure 2b presents the sulfoxide index, which remains relatively stable across various aging conditions but shows a slight increase during long-term aging (LTA). The pronounced sulfoxide peak can be attributed to the presence of sulfur- or silicate-containing groups in the fillers. Figure 2c depicts the hydroxyl index, which also rises with aging, indicating an accumulation of oxidative products. Longer PAV aging increases this index more than VBA-WET aging for W mastic, although the trend is similar for W60k mastic. Figures 2d and 2e display the long-chain index, which exhibits minimal changes under most aging conditions. However, a decrease is observed in the 783-838 cm⁻¹ region for W mastic during LTA, while the W60k sample remains relatively stable. The slight variations in the long-chain index may be influenced by the carbonate content in fillers such as limestone and carbonated hydrated lime.



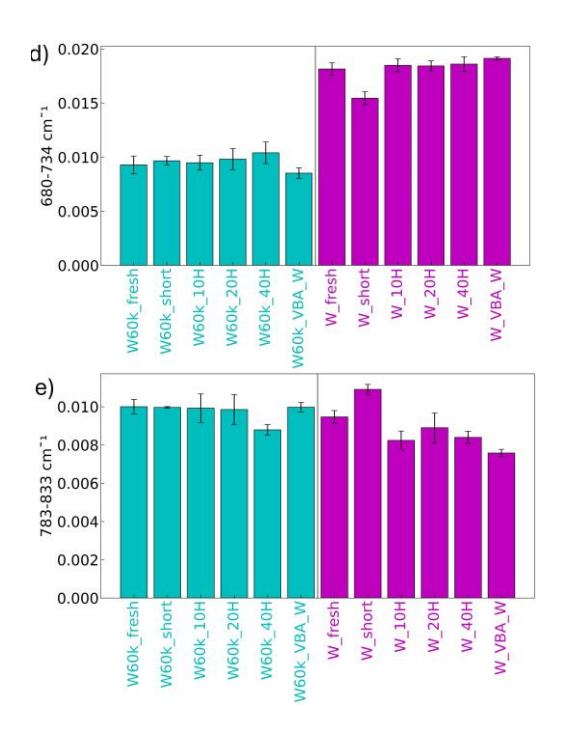


Figure 2- FTIR results for all samples: a) carbonyl index, b) sulfoxide index, c) hydroxyl index, d) 680-734 cm⁻¹, and e) 783-833 cm⁻¹, showing the effects of long-term aging under various conditions, including PAV (10, 20, and 40 hours) and VBA-WET aging.

3.2 Comparison of Mastic types

The comparison of W (limestone) and W60k (hydrated lime) mastics reveals significant differences in their aging behavior. For the carbonyl index (Figure 2a), both mastics exhibit similar trends under PAV aging; however, under VBA-WET conditions, W60k displays a lower carbonyl index, suggesting reduced oxidative aging due to the protective properties of hydrated lime. Regarding the sulfoxide index (Figure 2b), W60k consistently shows lower values compared to W mastic, likely attributable to differences in filler formulations. W60K also exhibits a smaller increase in the sulfoxide index after VBAwet aging than W, indicating reduced oxidative aging, similar to the carbonyl index trend. The hydroxyl index (Figure 2c) indicates a distinct peak for W60k mastic, reflecting the presence of OH functional groups in the filler, which is absent in W mastic. In the 680-734 cm⁻¹ region (Figure 2d), the longchain index is generally higher for W mastics, likely due to the greater carbonate content in limestone. Conversely, in the 783-838 cm⁻¹ region (Figure 2e), W60k mastic exhibits greater stability, with less degradation over time compared to W mastic, particularly under long-term aging and VBA-WET conditions. This suggests that W60k mastic is more resistant to oxidative and long-term aging. Further research is needed to validate these findings.

3.3 Mastic type analysis using PCA with indices vs. spectral data

This step aimed to compare the effectiveness of FTIR indices versus the entire FTIR spectra for analysing aging trends and sample classification. PCA was conducted separately on the FTIR indices and full spectra. The first two principal components explained over 80% of the variance for the indices and more than 70% for the spectra. A two-dimensional plot of PC1 versus PC2 (Figure 3) effectively represents the data. Figure 3 shows a clear distinction between W and W60k mastic samples in both FTIR indices and spectra-based PCA results, indicating that the preprocessing and index calculations retain essential information about sample type and aging behaviour. Both PC1 and PC2 are critical for differentiating the samples and tracking the aging process, with consistent aging trends observed in both analyses, characterized by a shift toward higher PC1 and lower PC2 values.

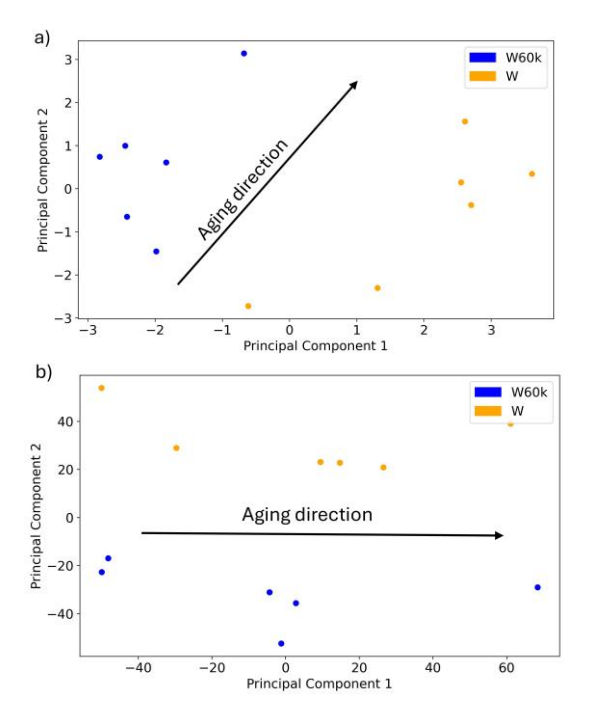


Figure 3- PCA plot of a) FTIR indices and b) FTIR spectra for fresh, short-term aged, and long-term aged mastic samples subjected to hygrothermal aging in PAV (10, 20, and 40 hours) and VBA-WET aging.

4 CONCLUSION

In conclusion, this study highlights the distinct aging behaviors of W (limestone) and W60k (hydrated lime) mastics, as revealed through FTIR analysis and PCA. The results demonstrate that W60k exhibits greater resistance to oxidative aging, particularly under VBA-WET conditions, as evidenced by lower carbonyl and sulfoxide indices. Additionally, the hydroxyl index indicates the presence of OH functional groups in W60k. The PCA results effectively

illustrate the differentiation between the two mastic types, confirming that both FTIR indices and spectra contain critical information essential for sample classification and aging assessment. Overall, these findings suggest that the choice of filler significantly impacts the aging behavior of mastics, and further research is warranted to explore the underlying mechanisms and implications for material performance in real-world applications.

5 ACKNOWLEDGMENT

The authors gratefully acknowledge the Dutch Ministry of infrastructure and Water Management for funding this project.

6 REFERENCE

Airey, G. D. 2003. State of the art report on ageing test methods for bituminous pavement materials. *International Journal of Pavement Engineering* 4(3): 165-176.

Alfaqawi, R. M., et al. 2022. Effect of hydrated lime and other mineral fillers on stiffening and oxidative ageing in bitumen mastic. *Construction and Building Materials* 315: 125789.

EN 12607-2, C. 2014. 12607-1: Bitumen and Bituminous Binders—Determination of the Resistance to Hardening under Influence of Heat and Air—Part 1: RTFOT Method. European Committee for Standardization: Brussels, Belgium

Gubler, R., et al. 1999. Investigation of the system filler and asphalt binders by rheological means. *Journal of the Association of Asphalt Paving Technologists* 68

Khalighi, S., et al. 2024a. Multivariate chemo-rheological framework for optimizing laboratory aging protocols of paving binders. *Materials & Design*: 113520.

Khalighi, S., et al. 2024b. The Impact of Reactive Oxygen Species Coupled with Moisture on Bitumen Long-Term Aging.

Khalighi, S., et al. 2024c. Evaluating the impact of data preprocessing methods on classification of ATR-FTIR spectra of bituminous binders. *Fuel* 376: 132701.

Khalighi, S., et al. 2025. Multi-scale analysis of ageing behaviour in bituminous materials.

Ma, L., et al. 2023. Chemical characterisation of bitumen type and ageing state based on FTIR spectroscopy and discriminant analysis integrated with variable selection methods. *Road Materials and Pavement Design*: 1-15.

Mastoras, F., et al. 2021. Effect of mineral fillers on ageing of bituminous mastics. *Construction and Building Materials* 276: 122215.

Migliori, F. and J.-F. Corté 1998. Comparative study of RTFOT and PAV aging simulation laboratory tests. *Transportation research record* 1638(1): 56-63.

Mirwald, J., et al. 2020. Impact of reactive oxygen species on bitumen aging—The Viennese binder aging method. *Construction and Building Materials* 257: 119495.

Petersen, J. C. 2009. A review of the fundamentals of asphalt oxidation: chemical, physicochemical, physical property, and durability relationships. *Transportation research circular*(E-C140)

Singhvi, P., et al. 2022. Impacts of field and laboratory long-term aging on asphalt binders. *Transportation Research Record* 2676(8): 336-353.